

Hydrodynamic Characteristics of Remora's Symbiotic Relationships

MARINE 2021

Yunxin Xu^{1*}, Weichao Shi² and Abel Arredondo-Galeana³

¹ Department of Naval Architecture, Ocean & Marine Engineering, University of Strathclyde, Henry Dyer Building, 100 Montrose Street, Glasgow G4 0LZ, UK., e-mail: yunxin.xu@strath.ac.uk

² Department of Naval Architecture, Ocean & Marine Engineering, University of Strathclyde, Henry Dyer Building, 100 Montrose Street, Glasgow G4 0LZ, UK., email: weichao.shi@strath.ac.uk

³ Department of Naval Architecture, Ocean & Marine Engineering, University of Strathclyde, Henry Dyer Building, 100 Montrose Street, Glasgow G4 0LZ, UK., email: abel.arredondo-galeana@strath.ac.uk

* Corresponding author: Yunxin Xu, Yunxin.xu@strath.ac.uk

ABSTRACT

Symbiotic relationships have developed through natural evolution which can provide advantages to parties in terms of survival. For example, that of the remora fish attached to the body of a shark to compensate for their poor swimming ability. From the remora's perspective, this could be associated to an increased hydrodynamic efficiency in swimming and this needs to be investigated. To understand the remora's swimming strategy in the attachment state, a systematic study has been conducted using the commercial Computational Fluid Dynamics CFD software, STAR-CCM+ to analyse and compare the resistance characteristics of the remora in attached swimming conditions. Two fundamental questions are addressed: what is the effect of the developed boundary layer flow and the effect of the adverse pressure gradient on the remora's hydrodynamic characteristics? By researching the hydrodynamic characteristics of the remora on varying attachment locations, the remora's unique behaviours could be applied to autonomous underwater vehicles (AUVs), which currently cannot perform docking and recovery without asking the mother vehicle to come for a halt.

Keywords: Remora fish; Computational Fluid Dynamics; Drag Reduction; Natural symbiotic

NOMENCLATURE

A	Reference area [m ²]
C_D	Drag coefficient
F	Drag force [N]
L	Reference length[m]
Re	Reynolds number
V	Incoming velocity [m s ⁻¹]
μ	dynamic viscosity of water [kg m ⁻¹ s ⁻¹]
ρ	Fluid density [kg m ⁻³]
CFD	Computational Fluid Dynamics

1. INTRODUCTION

The symbiotic relationships between different creatures in nature have been studied and developed to be applied in various fields. The behaviour of marine creatures such as the remora fish (e.g., *Echeneis neucratoides*, sometimes called “suckerfish”) where they attach to a host rather than swimming solo is a unique symbiotic relationship in the ocean. In fact, remora fish has a rather poor swimming ability, but using this “hitchhike” behaviour, they can travel over long distances (Michael Beckert *et al.*, 2016; M. Beckert *et al.*, 2015; Flammang *et al.*, 2020). The hosts of remora include a wide range of marine living creatures, such as sharks, turtles, as well as man-made marine vehicles.

On the top of the remora head, there is a suction disk for them to attach to a host. Many research studies have investigated this unique structure and tried to incorporate it into practical marine applications (M. Beckert *et al.*, 2015; Cohen *et al.*, 2020; Strasburg, 1962; Su *et al.*, 2020; Weihs *et al.*, 2007). Regarding to the attachment location, the location choice for remora is not random, and Brunnschweiler (Brunnschweiler, 2006) found that in total 345 cases nearly 39% of the attachment location choice is near the belly area of shark, followed by 27 % at the back and 21% at the pectoral fin. This phenomenon attracted a number of researchers to analyse the reasons for such behaviour. From a marine biology point of view, it was suspected that the remora typically selects a position that does not irritate the host (Silva-Jr & Sazima, 2006) and with minimal motion and deformation while the host is swimming in order to have a stable platform (Michael Beckert *et al.*, 2016). However, currently there is a lack of understanding about the hydrodynamic merits of selecting these attachment locations. Based on the study conducted by Brunnschweiler (Brunnschweiler, 2006), it was suggested that the remora fish favours attachment locations where adverse pressure gradients and developed boundary layers are present. But this has not been evidenced. Therefore, whether the remora fish selects its attachment location based on hydrodynamic benefits such as drag reduction needs to be investigated. By researching the motive and the potential benefits behind the behaviour of the remora, this concept could be applied to autonomous underwater vehicles (AUVs), which currently cannot perform docking and recovery without the mother vehicle being stationary.

Under this framework, the study researched into the hydrodynamic mechanism of the remora fish swimming to understand its behaviour from a hydrodynamic point of view. Firstly, based on the literature a generalised remora fish model and a shark model as the host are established. Then, the simulations in this study were divided into three groups for different conditions, which are the free-swimming case, the flat plate boundary layer case and the attachment case. For the free-swimming case, it mainly served as a reference case to set the benchmark and understand the hydrodynamic performance of the remora and the shark. Regarding the flat plate boundary layer case, the flat plate boundary layer case is to study the relationship between the drag on the remora and the independent variables, such as the boundary layer thickness and the associated Reynolds number. This study reveals the effect of boundary layer flow on the drag of remora fish, whereas the following study on the attachment locations reveals the effect of boundary layer flow in combination with the pressure gradient. By combining these three cases, comprehensive understandings can be achieved for remora’s hitchhiking behaviour.

2. CFD SIMULATION METHODOLOGY

2.1 Model Information and Geometry Preparation

According to the natural form and principal parameters of the remora and the shark living in the Puerto Rico sea area (CMS, 2019; Williams Jr *et al.*, 2003), the length of the remora fish model was selected to be an average size of 0.65m, and for the shark model, the length of model is 2m. The basic parameters of the models are presented in Fig. 1 and Fig.2.

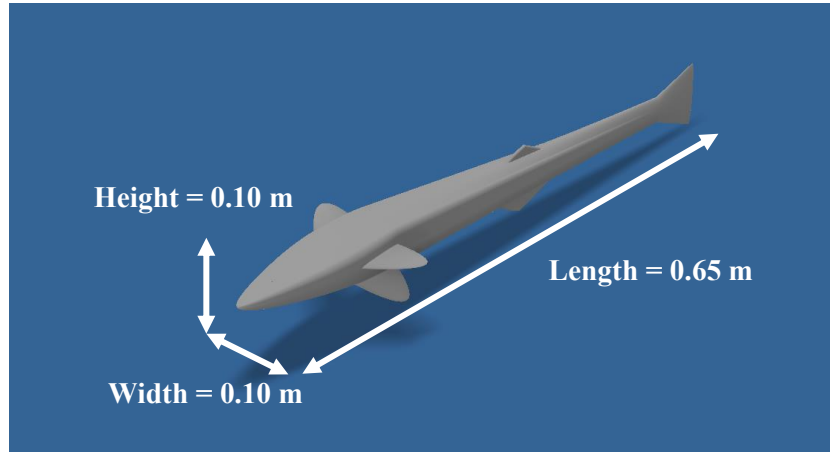


Figure 1. The 3D remora fish model for CFD simulation.

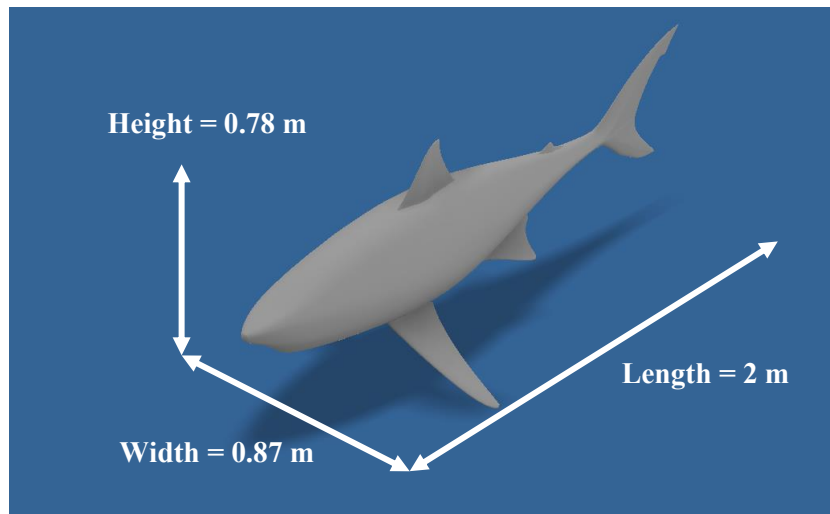


Figure 2. The 3D CAD oceanic whitetip shark model for CFD simulation.

For the attachment case, based on the results of experiments by Brunnschweiler *et al.* (Brunnschweiler, 2006), three favourable attachment locations (the belly, the back and the pectoral fin, as reproduced in Fig. 3) were chosen. Thus, as Fig. 4 shows, three CFD models were created that the remora attached to the shark at the different locations.

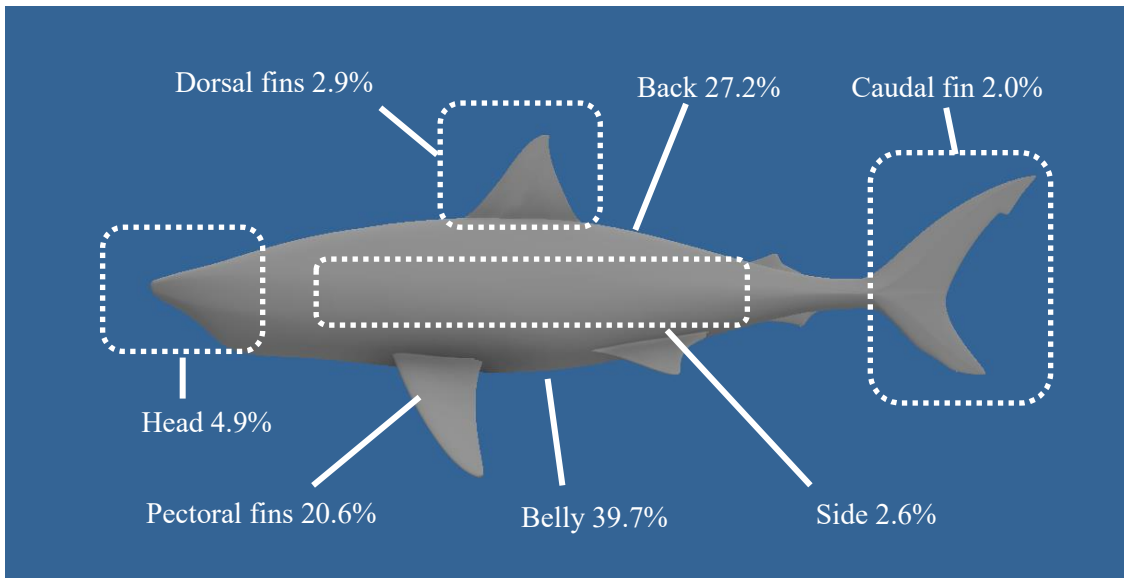


Figure 3. The probability that the remora attaches to the surface of shark at various locations (reproduced based on (Brunnschweiler, 2006)).

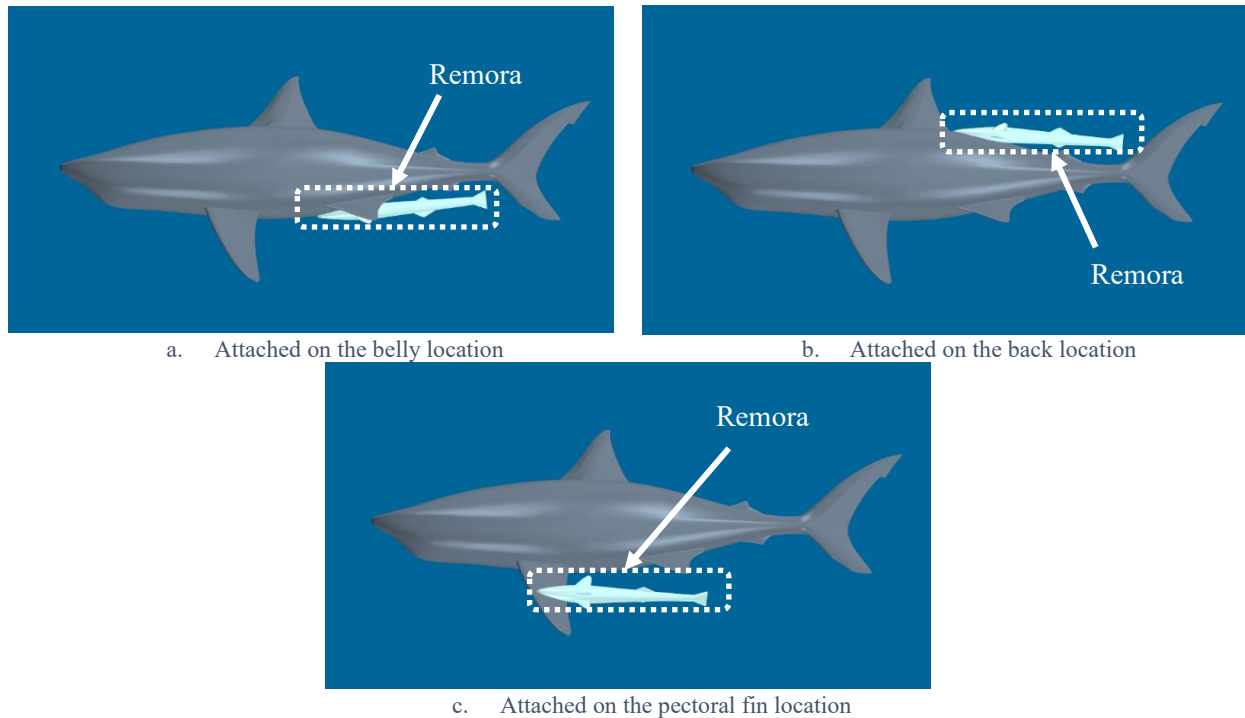


Figure 4. Attachment locations of the remora fish in the a) belly, b) back and c) pectoral fin of the shark.

2.2 CFD Simulation Setup

A Reynolds-averaged Navier–Stokes (RANS) model and a $K-\omega$ Shear Stress Transport ($K-\omega$ SST) turbulence model were chosen for this study (Singh *et al.*, 2011), and the all y^+ treatment was used in the simulations, which is a hybrid treatment to emulate the high- wall treatment for coarse meshes and the low- y^+ wall treatment for fine meshes(STAR-CCM+guidelines). The automatic meshing tool with volumetric control is used to generate the mesh. A more refined grid is used in the vicinity of the models which is about $0.1L$.

According to ITTC Practical Guidelines for Ship CFD Applications guidelines(ITTC, 2011), the dimensions of the computational domains are shown below in Fig. 5 and 6. Fig. 5 shows the computational domain is a cuboid domain that was selected for the free-swimming and attachment cases. The inlet boundary

is defined as the velocity inlet $5L$ upstream from the model, and the outlet boundary is defined as the pressure outlet $5L$ downstream from the model. The surrounding surfaces are positioned $1.5L$ from the model and are defined as the symmetry one. In addition, the shark and remora models are to be taken as no-slip wall.

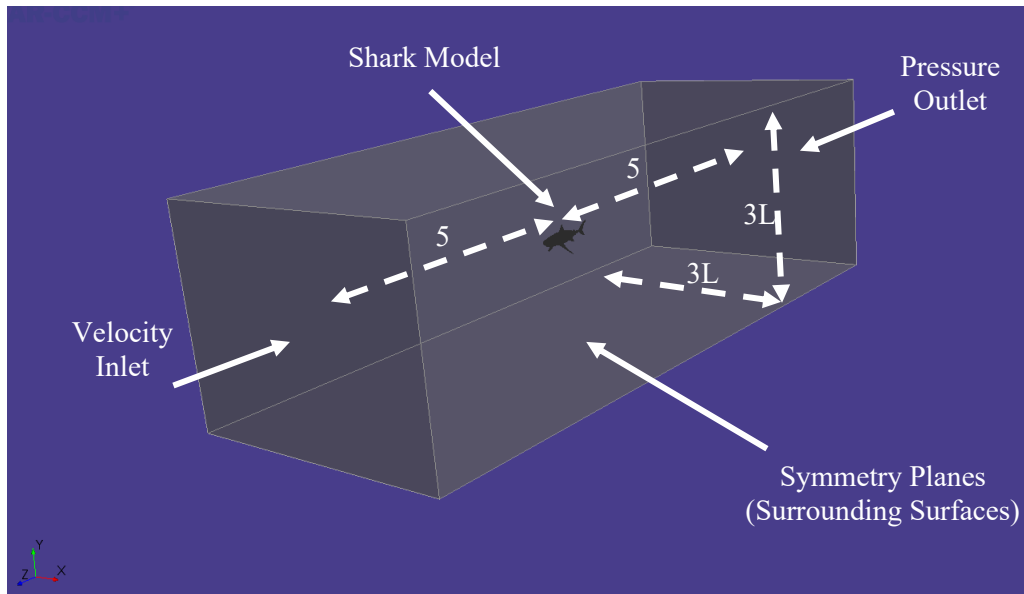


Figure 5. Domain and boundary conditions of the free-swimming and attachment cases.

Regarding the flat plate boundary layer case, the computational domain and boundary conditions are shown in Fig. 6. The outlet is defined as the pressure outlet $4L$ downstream from the model. The top and sides planes are set to be symmetry planes, and the height and the width of the domain are both $2L$. The inlet is defined as velocity inlet, and to introduce the different boundary layer thickness, the distance between the leading-edge and remora fish was set as $10m$, $20m$, $30m$, and $40m$. Meanwhile, the bottom plane (flat plate) and the remora model are set as no-slip wall conditions. In Fig. 6, the velocity inlet boundary is positioned $10m$ upstream from the model.

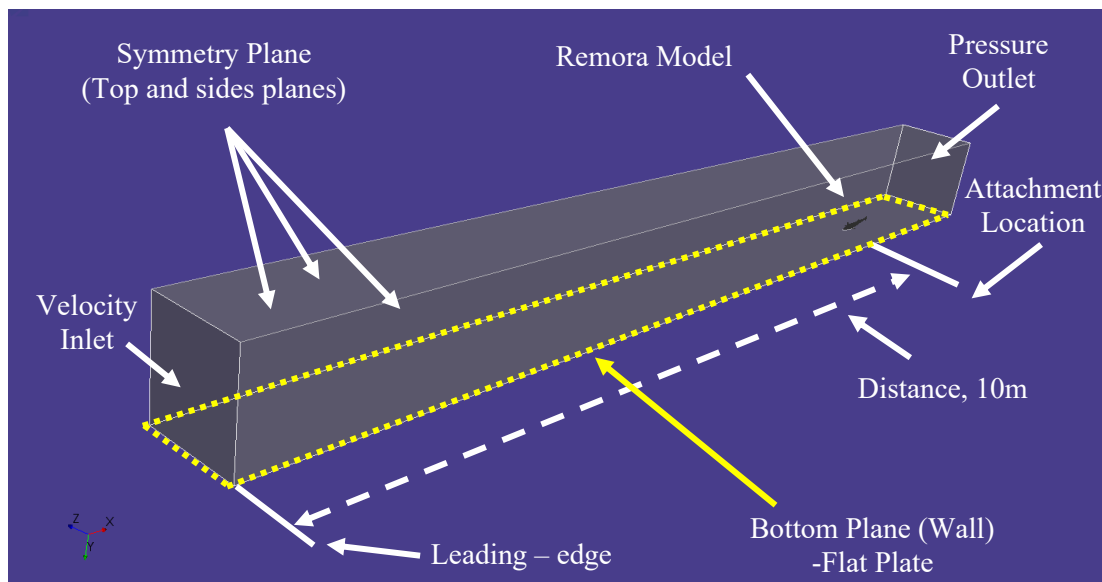


Figure 6. Domain and boundary conditions of the flat plate boundary layer case.

3. RESULT ANALYSIS AND DISCUSSION

3.1 Free-swimming case

Numerical simulations were performed with the CFD software STAR-CCM+ to investigate the hydrodynamic free-swim characteristics of the remora and the shark and to set out our benchmark cases. The average speed of the oceanic whitetip shark ranges between 1kn to 8kn (Papastamatiou *et al.*, 2018) and the remora can experience the same speed through attaching to the shark. Therefore, in this case, the velocities of the shark and remora are both set to vary from 1kn to 8kn.

In this section, the nondimensional number is used to compare the resistance performance at different velocities for the remora and shark. The Reynolds number, Re , is calculated with the following equation (1):

$$Re = \frac{\rho * L * V}{\mu}, \quad (1)$$

where, ρ is the density of the water, 997kg/m³; L is the reference length, m; V is the incoming velocity, m/s; μ is the dynamic viscosity of water, 0.001kg/(ms).

And the drag coefficient, C_D , is calculated with the following equation (2):

$$C_D = \frac{F}{\frac{1}{2} * \rho * V^2 * A}, \quad (2)$$

where, F is the drag force, N; A is the reference frontal area of the model (width * height, m²).

The drag coefficients results are shown in Fig. 7. It can be seen that at the same velocity, the remora fish has a much lower Reynolds number than the shark due to the different body lengths. However, under the same Reynolds number, the drag coefficient of the remora is much higher than the one of the shark. Therefore, in its free-swimming mode, the remora fish does not show any competitive drag performance.

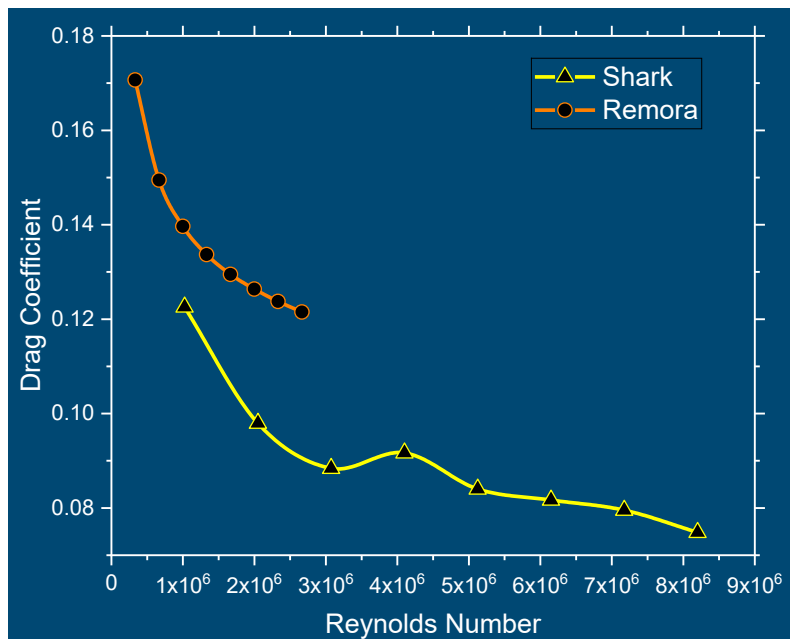


Figure 7. Drag coefficients vs. Reynolds numbers of remora and shark in free-swimming.

To further investigate the hydrodynamic characteristics of both remora and shark in free-swimming condition, the velocity contours in the mid-section and the pressure contours on the body have been extracted. Because the contours between different velocities are similar, the 8kn inflow velocity case of the shark is displayed in Fig. 8. As Fig.8 shows, the adverse pressure gradient regions with low flow velocity develop after the belly and the back regions due to the dorsal fin and bulky body of the shark. This hydrodynamic characteristic of the attachment locations which the remora prefers could be a clue for the following study.

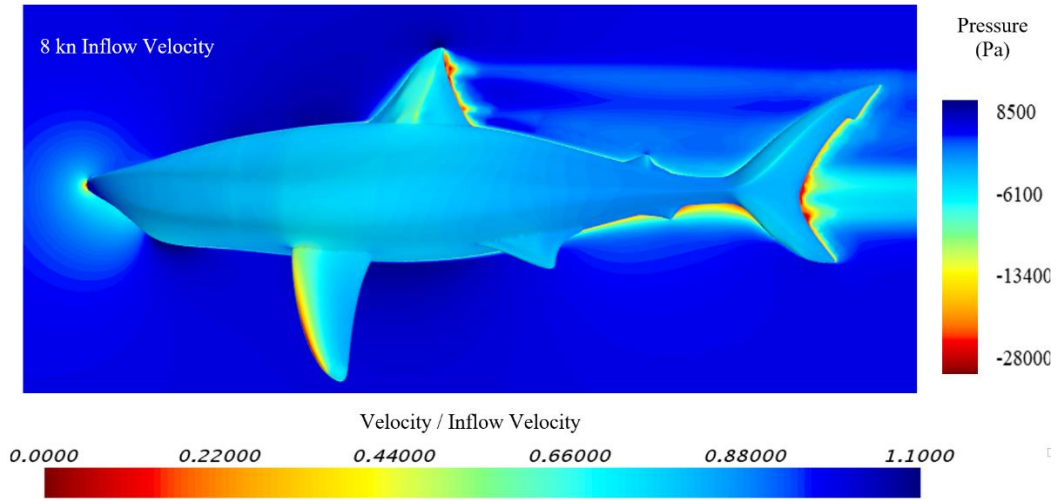


Figure 8. Velocity and pressure contours of the shark in free-swimming condition (Pressure contour displayed on the surface of model, and velocity contours displayed on the section plane).

3.2 Flat plate boundary layer case

By computing the drag on the remora which is covered by the flat plate boundary layer flow, this section focuses on investigating the effect of the developed boundary layer flow on the remora fish. In this case, the incoming flow velocity was set as 4kn. There are four remora attachment locations, and its distance is varied between 10m, 20m, 30m, and 40m downstream from the leading edge of the flat plate. The results were shown in Fig. 9.

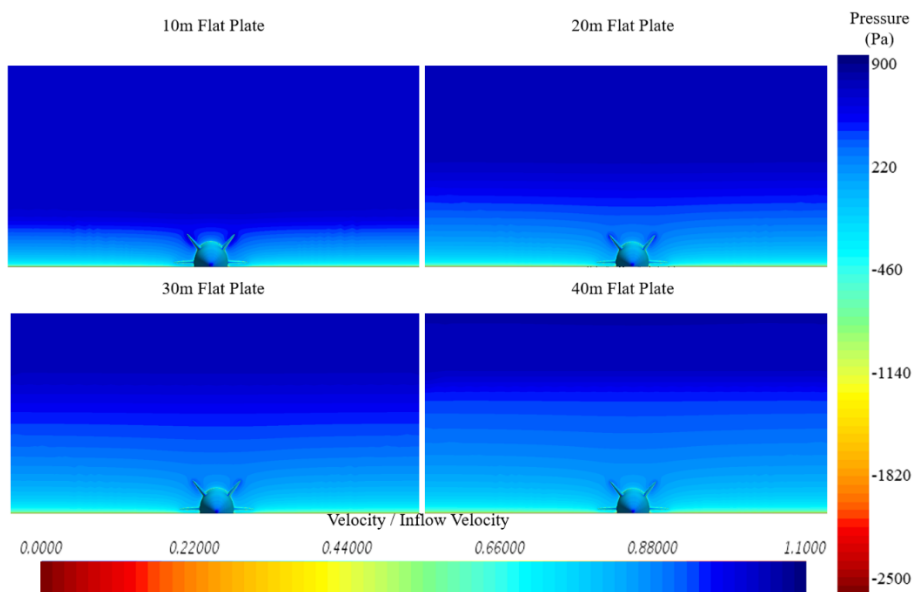


Figure 9. The velocity contour on the cross-section and pressure contour on the remora fish (Pressure contour displayed on the surface of model, and velocity contours displayed on the section plane).

From the drag results in the free-swimming case, when the developed boundary layer flow covered the remora, a drag reduction on the remora can be seen. Meanwhile, the drag reduction increase from 27% to 36% with the increased boundary layer thickness (based on the length of the flat plate) as shown in Fig. 10. Therefore, from a drag reduction point of view, in order to lower drag on the body, the remora fish tend to attach a region where is covered a developed boundary layer.

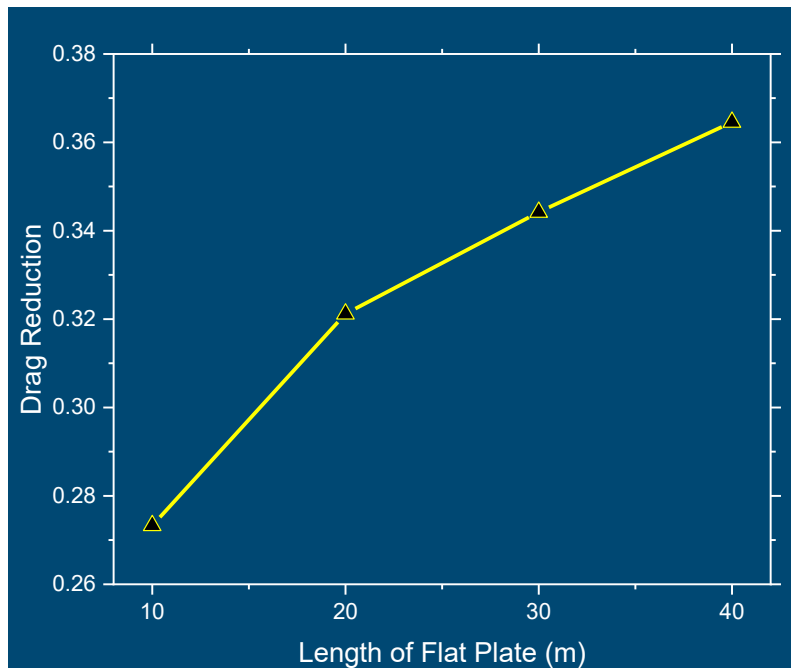


Figure 10. The drag reduction rate vs. the length of the flat plate.

3.3 Attachment case

After the above simulations, the hydrodynamic characteristics of the remora attaching to the different location of the shark’s surface are analysed in this section. Three attachment location (belly, back and pectoral fin) are chosen to compute at 8kn, and the drag reduction rate for remora can be obtained by comparing the results of the free-swimming condition (section 3.1), which is shown below Table 1. Meanwhile, the velocity contour on the section and the pressure contour on the surface both are extracted as shown in Fig. 11, Fig. 12, and Fig. 13.

Table 1. The drag reduction rate of remora fish attaching to different locations.

Location	Belly	Back	Pectoral fin
Drag Reduction Rate	58%	69%	29%

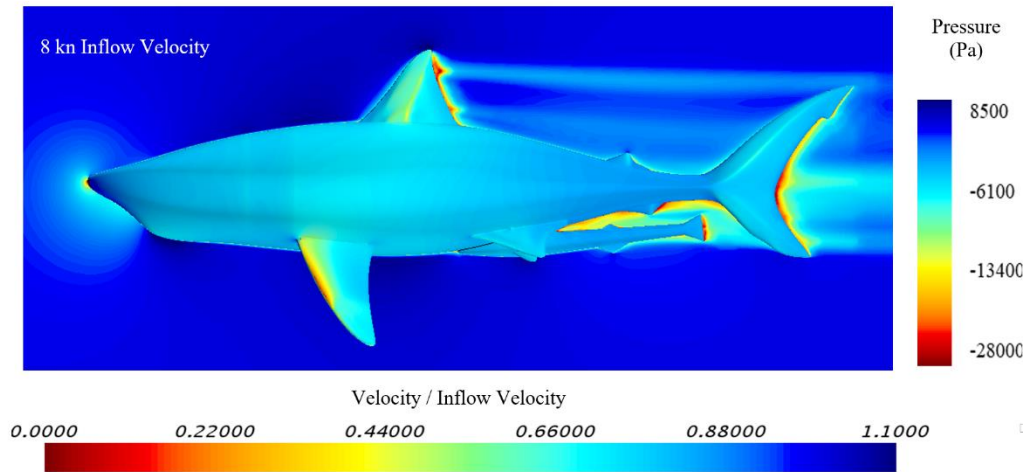


Figure 11. Velocity and pressure contours of the remora attached to the belly of the shark (Pressure contour displayed on the surface of model, and velocity contours displayed on the section plane).

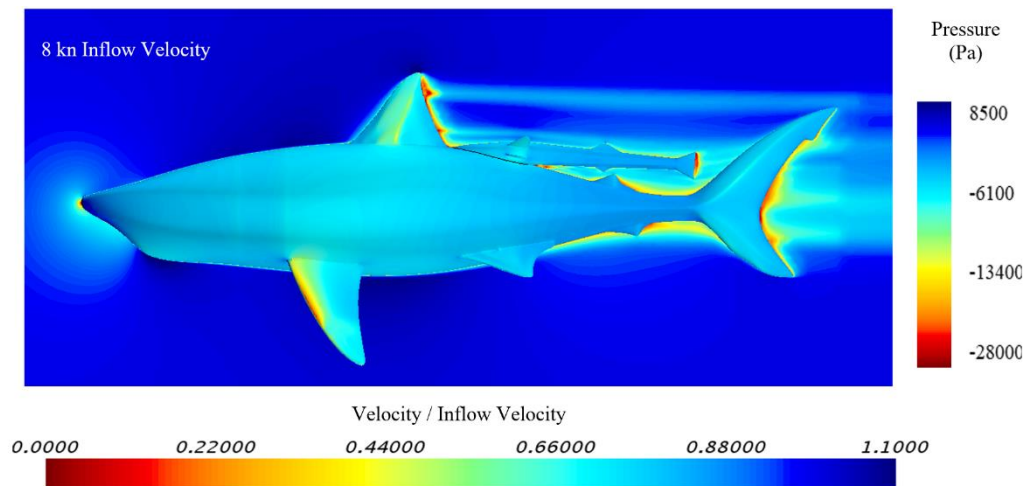


Figure 12. Velocity and pressure contours of the remora attached to the back of the shark (Pressure contour displayed on the surface of model, and velocity contours displayed on the section plane).

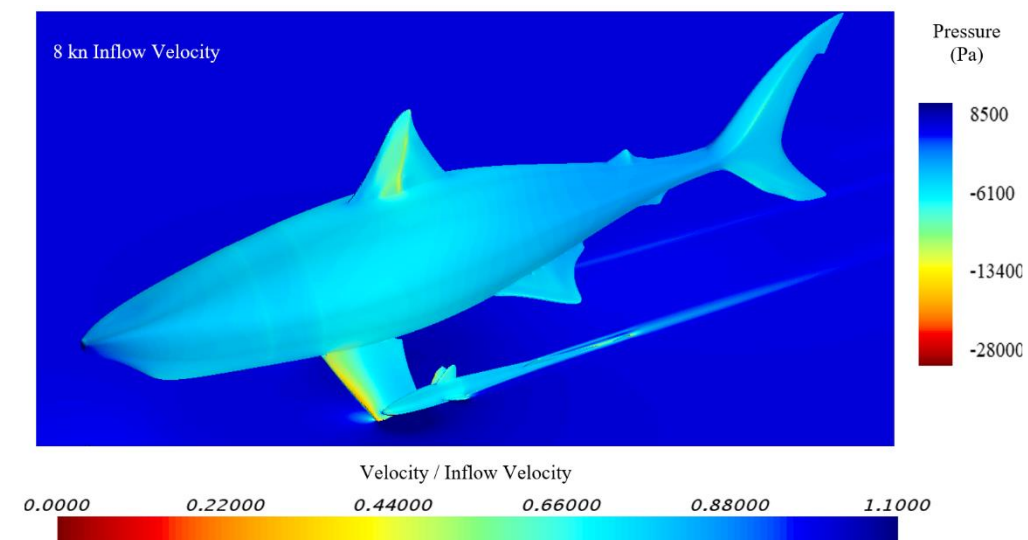


Figure 13. Velocity and pressure contours of the remora attached to the pectoral fin of the shark (Pressure contour displayed on the surface of model, and velocity contours displayed on the section plane).

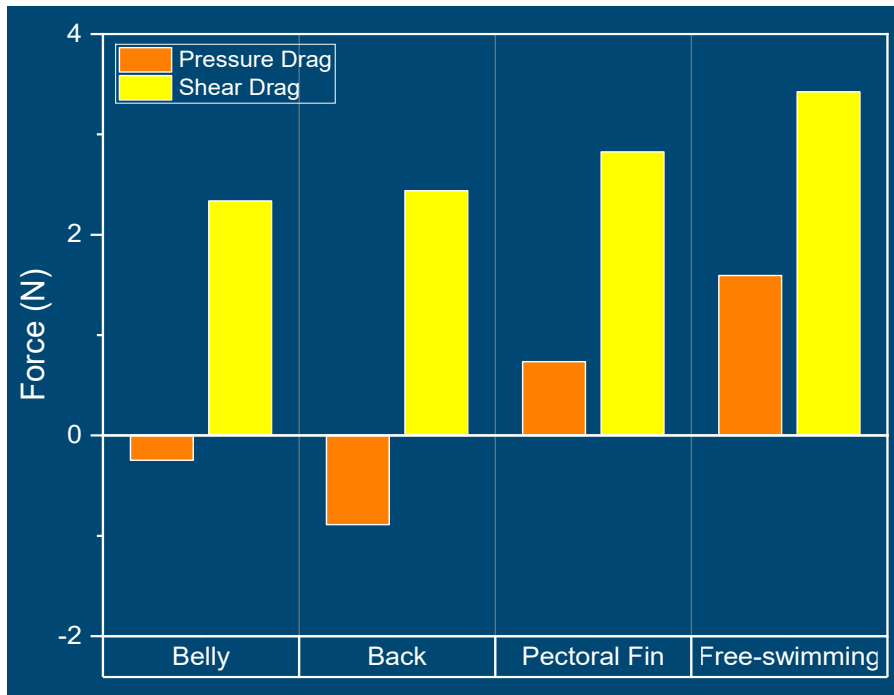


Figure 14. Comparisons of the pressure forces and the shear forces for remora.

The drag components of the remora (pressure drag and shear drag) for the free-swimming condition and the different attachment locations are shown in Fig. 14. Combined with the results of attachment condition which are shown in Fig.11, Fig.12, and Fig.13, the effect of the attachment location on the surface of the shark for the remora fish are discussed following:

Firstly, Fig. 11 shows the belly attachment case, there is a low-velocity area around the remora, and this region is also in an adverse pressure gradient area which builds up due to the blockage of the shark body. Therefore, the belly attachment case shows the lowest shear drag relative to other attachment locations. In addition, it is worth noticing that the pressure force provides a forward thrust to remora, which demonstrated the effect of the adverse pressure gradient.

Secondly, the back attachment case is shown in Fig.12. it can be seen that behind the dorsal fin there is a larger adverse pressure region due to the slope of the shark back and the dorsal fin, thus the pressure force provides a higher forward thrust than the one in the belly attachment case. Therefore, from the belly and back attachment case, it can be confirmed that the low velocity and the adverse pressure gradient area can provide a higher drag reduction rate for the remora.

Finally, regarding the pectoral fin attachment location, the pectoral fin of shark blocks a part of incoming flow, and however, most of the remora body is exposed to the incoming flow. Meanwhile, around the remora body, there are the high-velocity and high-pressure regions. Hence, in this attachment location the drag reduction rate is the lowest.

4. CONCLUSIONS

An investigation has been conducted to study the hydrodynamic characteristics of the remora fish in attached swimming conditions. This research has primarily focused on the investigations of the effect of the developed boundary layer flow and the effect of the different attachment locations on the shark body for the remora.

Regarding the effect of boundary layer flow on the remora fish, it can be seen that the drag reduction rate is related to the boundary layer thickness. In terms of the attachment locations, the most frequent locations are the belly, the back and the pectoral fin of the shark. It is found that the belly and the back locations are the

regions with the lowest velocities and adverse pressure gradient regions. Therefore, not only the boundary layer but also the flow characteristics in the attachment locations are determining factors in the drag reduction rate of the remora.

Future development will focus to complete the simulations. One is the effect of the inflow velocity should be considered in the flat plate boundary layer case. Another one is about the attachment case. The more inflow velocities will be simulated to analyse the effect of velocity on the pressure drag and shear drag. Meanwhile, the variation of the drag on the shark body also will be studied.

ACKNOWLEDGEMENTS

Results were obtained using the ARCHIE-WeSt High Performance Computer (www.archie-west.ac.uk) based at the University of Strathclyde.

REFERENCES

- Beckert, M., Flammang, B. E., Anderson, E. J., & Nadler, J. H. (2016). Theoretical and computational fluid dynamics of an attached remora (*Echeneis naucrates*). *Zoology*, *119*(5), 430-438.
- Beckert, M., Flammang, B. E., & Nadler, J. H. (2015). Remora fish suction pad attachment is enhanced by spinule friction. *J Exp Biol*, *218*(Pt 22), 3551-3558. doi:10.1242/jeb.123893
- Brunnschweiler, J. M. (2006). Sharksucker-shark interaction in two carcharhinid species. *Marine Ecology*, *27*(1), 89-94. doi:10.1111/j.1439-0485.2005.00052.x
- CMS. (2019). Puerto Rico (USA). Retrieved from <https://www.cms.int/sharks/en/country/puerto-rico-usa>
- Cohen, K. E., Flammang, B. E., Crawford, C. H., & Hernandez, L. P. (2020). Knowing when to stick: touch receptors found in the remora adhesive disc. *R Soc Open Sci*, *7*(1), 190990. doi:10.1098/rsos.190990
- Flammang, B. E., Marras, S., Anderson, E. J., Lehmkuhl, O., Mukherjee, A., Cade, D. E., . . . Vázquez, M. (2020). Remoras pick where they stick on blue whales. *Journal of Experimental Biology*, *223*(20).
- ITTC. (2011). *Practical guidelines for ship CFD applications*. Paper presented at the 26th ITTC, Hague.
- Papastamatiou, Y. P., Iosilevskii, G., Leos-Barajas, V., Brooks, E. J., Howey, L. A., Chapman, D. D., & Watanabe, Y. Y. (2018). Optimal swimming strategies and behavioral plasticity of oceanic whitetip sharks. *Sci Rep*, *8*(1), 551. doi:10.1038/s41598-017-18608-z
- Silva-Jr, J. M., & Sazima, I. (2006). Whalesuckers on spinner dolphins: an underwater view. *JMBA2–Biodiversity Records*.
- Singh, H., Fletcher, D. F., & Nijdam, J. J. (2011). An assessment of different turbulence models for predicting flow in a baffled tank stirred with a Rushton turbine. *Chemical Engineering Science*, *66*(23), 5976-5988.
- STAR-CCM+guidelines. STAR-CCM+ Documentation.
- Strasburg, D. W. (1962). Some aspects of the feeding behavior of *Remora remora*.
- Su, S., Wang, S., Li, L., Xie, Z., Hao, F., Xu, J., . . . Wen, L. (2020). Vertical Fibrous Morphology and Structure-Function Relationship in Natural and Biomimetic Suction-Based Adhesion Discs. *Matter*, *2*(5), 1207-1221. doi:10.1016/j.matt.2020.01.018

- Weih, D., Fish, F. E., & Nicastro, A. J. (2007). Mechanics of Remora Removal by Dolphin Spinning. *Marine Mammal Science*, 23(3), 707-714. doi:10.1111/j.1748-7692.2007.00131.x
- Williams Jr, E. H., Mignucci - Giannoni, A. A., Bunkley - Williams, L., Bonde, R. K., Self - Sullivan, C., Preen, A., & Cockcroft, V. G. (2003). Echeneid - sirenian associations, with information on sharksucker diet. *Journal of Fish Biology*, 63(5), 1176-1183.